BIOMOLECULES & THERAPEUTICS

Original Article
Biomol Ther 33(3), 483-493 (2025)

1,3,5-Tricaffeoylquinic Acid from *Ipomoea batatas* Vines Induced Ovarian Cancer Cell Apoptosis and Inhibited Endothelial Tube Formation

Dahae Lee[1,†], Jaekyoung Kim[2,†], Soyoon Baek[3], Jin Woo Lee[4], Changyeol Lee[5], Ki Sung Kang[1,*] and Sang Hee Shim[2,*]

[1]*College of Korean Medicine, Gachon University, Seongnam 13120,*
[2]*Natural Products Research Institute, College of Pharmacy, Seoul National University, Seoul 08826,*
[3]*R&D Complex, Kolmar Korea, Seoul 06800,*
[4]*College of Pharmacy, Duksung Women's University, Seoul 01369,*
[5]*Herbal Medicine Resources Center, Korea Institute of Oriental Medicine, Naju 58245, Republic of Korea*

Abstract

Ovarian cancer usually metastasizes from the ovary to adjacent organs through direct invasion with blood vessels formed by endothelial cells. Targeting apoptosis of ovarian cancer and angiogenesis is promising for anticancer therapy. Leaves of *Ipomoea* sp. have reportedly shown promise in treating ovarian cancer. Here, we investigated the apoptosis-inducing and anti-angiogenic effects of compounds isolated from *Ipomoea batatas* vines (IBV). Phytochemical examination of IBV led to the isolation and verification of eight compounds (**1-8**): chlorogenic acid (**1**), 3,4-dicaffeoylquinic acid (**2**), 3,5-dicaffeoylquinic acid (**3**), 4,5-dicaffeoylquinic acid (**4**), 1,3,5-tricaffeoylquinic acid (**5**), *N-trans*-feruloyltyramine (**6**), scopoletin (**7**), and esculetin (**8**). Of these, 1,3,5-tricaffeoylquinic acid (**5**) showed the highest cytotoxicity in A2780 human ovarian cancer cells, inducing apoptotic death in more than 37% cells and decreasing viability to less than 25% at 100 μM. Compound **5** increased the levels of cleaved caspase-8, Bax, cleaved PARP, and caspase-3/9, and decreased the levels of cleaved Bcl-2. Further, **5** inhibited tubule formation in HUVECs. VEGFR2, ERK, PI3K, Akt, and mTOR protein expression was also suppressed by **5**. Then, a simple, rapid, and reliable LC-MS/MS method was developed to determine the contents of the isolated compounds from IBV. Overall, **5** has potential for treating ovarian cancer as it induces apoptosis in ovarian cancer cells and inhibits tube formation.

Key Words: *Ipomoea batatas* vines, 1,3,5-tricaffeoylquinic acid, Ovarian cancer, Apoptosis, LC-MS/MS

INTRODUCTION

Ipomoea batatas or 'sweet potato,' is an herbaceous perennial vine belonging to the Convolvulaceae family. Its vines, roots, and leaves are used as popular food sources worldwide (Zhang *et al*., 2019). In both humans and animals, they provide a significant source of energy and phytochemicals (Mohanraj and Sivasankar, 2014). Owing to their therapeutic properties, including treatment of prostatitis. *I. batatas* vines (IBV) in particular have been used in traditional medicine (Noumi, 2010). IBV has been utilized as a common dish in Korea for a very long time. To date, more than 135 compounds have been isolated and identified from the leaf, root, and skin extracts of *Ipomoea batatas*, including 47 flavonoids, 36 phenolic acids, 18 organic acids, 14 carotenoids, and others (sesquiterpenes, monoterpenes, alkaloids, and triterpenols) (Jiang *et al*., 2022). Ovarian cancer is a dangerous disease for women because it is often diagnosed at an advanced stage (III and IV) (Doubeni *et al*., 2016). It is particularly lethal for women of childbearing age (Zanetta *et al*., 1997). Platinum- and taxane-based chemotherapy after surgery is the most effective treatment for ovarian cancer; however, less than 20% of patients show beneficial responses to these chemotherapies (Markman *et al*., 2004), as they can lead to drug resistance. Therefore,

Open Access **https://doi.org/10.4062/biomolther.2024.239**

Received Dec 11, 2024 **Revised** Jan 20, 2025 **Accepted** Jan 28, 2025
Published Online Apr 8, 2025

***Corresponding Authors**
E-mail: sanghee_shim@snu.ac.kr (Shim SH),
kkang@gachon.ac.kr (Kang KS)
Tel: +82-2-901-8774 (Shim SH), +82-31-750-5402 (Kang KS)
Fax: +82-31-750-5416 (Kang KS)
[†]The first two authors contributed equally to this work.

developing ovarian cancer treatments that are both efficient and tolerable over the long term is crucial. Typically, ovarian cancer spreads from the ovary to nearby organs through direct invasion of blood vessels, which are composed of endothelial cells.[8] Thus, apoptosis-based therapies that regulate unchecked cancer cell division and angiogenesis-based therapies that prevent cancer cell metastasis are of significant interest (Reed, 2002; Scappaticci, 2002). Several plant-derived bioactive substances have been found to be effective against metastatic cancer (Pezzuto, 1997; Pistollato *et al*., 2015; Al-Alem *et al*., 2019; Roy *et al*., 2021).

It may thus be worthwhile to explore anticancer compounds from IBV based on the findings from other parts of this plant (Mohanraj and Sivasankar, 2014). Consequently, the goal of this study was to identify phytochemicals that could prevent or treat ovarian cancer by inhibiting tube formation in human umbilical vein endothelial cells (HUVECs) or inducing death in human ovarian cancer cells (A2780). The effects of these compounds on the viability and apoptosis of A2780 cells was examined. Further, the compound with the highest cytotoxicity was assessed in the HUVEC tube formation assay.

Several methods have been developed to determine compounds from the tubers of purple sweet potatoes. For instance, chlorogenic acid derivatives such as mono-, di-, and tri-caffeoyl quinic acids, have been isolated from the leaves of *I. batatas* and quantified using HPLC-UV (Islam *et al*., 2002). However, the LC-ESI-MS/MS-based simultaneous quantification approach used in this study has not been used previously. Overall, this study covers the structural characterization of compounds **1-8**, their anticancer potential, the underlying molecular pathways, and the development of a quantitative technique.

MATERIALS AND METHODS

General experimental procedures

Nuclear magnetic resonance (NMR) spectra were obtained using Varian NMR systems 500 MHz (^{1}H: 500 MHz, ^{13}C: 125 MHz) (Varian, Palo Alto, CA, USA) with CD_3OD (Cambridge Isotope Laboratories, Inc., Tewksbury, MA, USA). Chemical shifts were referenced to a residual solvent signal CD_3OD (δ_H 3.31). Waters Millipore 600 system equipped with a binary pump and 996 PDA detector. It was performed on Luna 5 um C_{18}(2) column (250 mm×10 mm, Phenomenex, Torrance, CA, USA). UPLC-ESI-MS/MS spectra were acquired using a Vanquish Flex liquid UHPLC system (Thermo, CA, USA) and LTQ XL mass spectrometer (Thermo) equipped with electrospray source and capable of analyzing ions up to m/z 2000. It was performed on Hypersil GOLD C_{18}(2) column (150 mm×2.1 mm, Phenomenex). Mass spectrometer were optimized in order to achieve maximum sensitivity.

Plant materials

The vines of *I. batatas* were provided by Prof. Dongho Kang of Kyung Hee University in August 2019. Voucher specimens (NPC-16-08NF) were deposited at the Natural Products Research Institute, College of Pharmacy, Seoul National University, Seoul, Korea.

Extraction and isolation

I. batatas vines (443 g) were extracted thrice with 100% methanol and then evaporated under reduced pressure to yield an extract (130 g). The crude extract was fractionated using vacuum liquid chromatography over Diaion HP20 with a stepwise gradient of water-acetone to obtain 10 fractions (fractions 1-10). Fraction 2 (1.22 g) was loaded on a C_{18} medium-pressure column chromatograph (MPLC) to separate fractions 2A to 2L, which were eluted using a gradient of water-MeOH. Fraction 2C (54.5 mg) was subjected to reversed-phase high-pressure liquid chromatography (HPLC) [Phenomenex, Luna C_{18} (2), 5 μm, 250×10 mm, isocratic aqueous 65% CH_3CN, 2.0 mL/min] to isolate **7** (1.0 mg). Fraction 2E (34 mg) was isolated using reverse-phase HPLC (Phenomenex, Luna C_{18} (2), 5 μm, 250×10 mm, isocratic aqueous 65% CH_3CN, 2.0 mL/min) to obtain **8** (1.6 mg). Fraction 2G was separated into seven fractions (Fraction 2G1-2G7) by normal phase MPLC using a gradient of CHCl3-MeOH. Fraction 2G3 was further separated using reverse-phase HPLC (Phenomenex, Luna C_{18} (2), 5 μm, 250×10 mm, isocratic aqueous 65% CH_3CN, 2.0 mL/min) to yield **2** (3.3 mg), **3** (17 mg), **4** (6.1 mg), and **5** (7.7 mg). Fraction 3 (480 mg) was separated into nine fractions (Fraction 3A-3I) by normal-phase MPLC using a gradient of hexane-EtOAc-MeOH. Fraction 3E was then subjected to reverse-phase HPLC (Phenomenex, Luna C_{18} (2), 5 μm, 250×10 mm, isocratic aqueous 65% CH_3CN, 2.0 mL/min) to isolate 6 (1.6 mg).

Chlorogenic acid (**1**): ^{1}H NMR (CD_3OD, 400 MHz) δ 7.57 (d, *J*=15.5 Hz), 7.03 (d, *J*=1.5 Hz), 6.98 (dd, *J*=8.0, 1.5 Hz), 6.77 (dd, *J*=8.0, 1.5 Hz), 6.29 (d, *J*=15 Hz), 5.36 (m), 4.13 (m), 3.66 (m), 2.18 (m), 2.13 (m), 1.94(m); (+)ESIMS *m/z* 347.2 $[M+H]^+$.

3,4-Dicaffeoylquinic acid (**2**): yellowish, amorphous solid; ^{1}H NMR (CD_3OD, 500 MHz) δ 7.47 (d, *J*=15.5 Hz), 7.54 (d, *J*=16 Hz), 7.04 (d, *J*=1.5 Hz), 7.02 (d, *J*=1.5 Hz), 6.93 (dd, *J*=8.0, 1.5 Hz), 6.88 (dd, *J*=8.5, 1.5 Hz), 6.77 (d, *J*=8.5 Hz), 6.73 (d, *J*=8.5 Hz), 6.29 (d, *J*=15.5 Hz), 6.26 (d, *J*=16 Hz), 5.63 (m), 5.00 (m), 4.35 (m), 2.11-2.28 (m), 2.11-2.28 (m); (+) ESIMS *m/z* 517.4 $[M+H]^+$.

3,5-Dicaffeoylquinic acid (**3**): yellowish, amorphous solid; ^{1}H NMR (CD_3OD, 500 MHz) δ 7.61 (d, *J*=16 Hz), 7.58 (d, *J*=16 Hz), 7.04 (d, *J*=1.5 Hz), 7.02 (d, *J*=1.5 Hz), 6.93 (dd, *J*=8.5, 1.5 Hz), 6.88 (dd, *J*=8.5, 1.5 Hz), 6.73 (d, *J*=8.5 Hz), 6.36 (d, *J*=16 Hz), 6.27 (d, *J*=16 Hz), 5.42 (m), 5.38 (m), 3.90 (m), 2.32 (m), 2.21-2.24 (m); (+)ESIMS *m/z* 517.3 $[M+H]^+$.

4,5-Dicaffeoylquinic acid (**4**): yellowish, amorphous solid; ^{1}H NMR (CD_3OD, 500 MHz); δ 7.57 (d, *J*=16 Hz), 7.54 (d, *J*=16 Hz), 7.04 (d, *J*=1.5 Hz), 7.02 (d, *J*=1.5 Hz), 6.93 (dd, *J*=8.5, 1.5 Hz), 6.88 (dd, *J*=8.5, 1.5 Hz), 6.77 (d, *J*=8.5 Hz), 6.73 (d, *J*=8.5 Hz), 6.28 (d, *J*=16 Hz), 6.25 (d, *J*=16 Hz), 5.62 (m), 5.11 (m), 4.35 (m), 2.25 -1.97 (m); (+)ESIMS *m/z* 517.5 $[M+H]^+$.

1,3,5-Tricaffeoylquinic acid (**5**): yellowish, amorphous solid; ^{1}H NMR (CD_3OD, 500 MHz) δ 7.64 (d, *J*=16 Hz), 7.51 (d, *J*=15.5 Hz), 7.50 (d, *J*=16 Hz), 7.06 (d, *J*=1.5 Hz), 6.98 (d, *J*=1.5 Hz), 6.96 (dd, *J*=8.0, 1.5 Hz), 6.84 (d, *J*=1.5 Hz), 6.81 (dd, *J*=8.0, 1.5 Hz), 6.78 (d, *J*=8.0 Hz), 6.64 (d, *J*=8.0 Hz), 6.64 (dd, *J*=8.0, 1.5 Hz), 6.53 (d, *J*=8.5 Hz), 6.33 (d, *J*=16 Hz), 6.25 (d, *J*=16 Hz), 6.18 (d, *J*=15.5 Hz), 5.57 (m), 5.45 (m), 3.99 (m), 2.42-2.90 (m), 2.00-2.67 (m); (+)ESIMS *m/z* 679.5 $[M+H]^+$.

N-trans-feruloyltyramine (**6**): yellowish, amorphous solid; ^{1}H NMR (CD_3OD, 500 MHz) δ 7.43 (d, *J*=15.5 Hz), 7.12 (d, *J*=1.5 Hz), 7.05 (d, *J*=8.5 Hz), 7.02 (dd, *J*=8.0, 1.5 Hz), 6.79 (d, *J*=8.0 Hz), 6.71 (d, *J*=8.3 Hz), 6.40 (d, *J*=15.5 Hz), 3.88 (s), 3.46 (t, *J*=7.5 Hz), 2.74 (t, *J*=7.5 Hz); (+)ESIMS *m/z* 314.3 $[M+H]^+$.

Scopoletin (**7**): yellowish, amorphous solid; ^{1}H NMR

Table 1. Conditions for LC-MS/MS analysis of IBV compounds

HPLC condition			
Column	Thermo UPLC gold C_{18} (150×2.1 mm, 1.9 um)		
Flow rate	0.3 mL/min		
Injection volume	5.0 uL		
Column temperature	30℃		
Sample temperature	20℃		
Mobile phase	Time	A	B
	0	90	10
	5	70	30
	10	0	100
	11	90	10
	15	90	10
MS condition			
Capillary voltage (kV)	4.5		
Source temp. (℃)	300℃		
Capillary temp. (℃)	320℃		

(CD_3OD, 500 MHz) δ 7.87 (d, *J*=9.5 Hz), 7.12 (s), 6.78 (s), 6.21 (d, *J*=9.5 Hz), 3.91 (s); (+)ESIMS *m/z* 193.1 $[M+H]^+$.

Esculetin (**8**): yellowish, amorphous solid; ^1H NMR (CD_3OD, 500 MHz) δ 7.78 (d, *J*=9 Hz), 6.94 (s), 6.75 (s), 6.18 (d, *J*=9 Hz); (+)ESIMS *m/z* 179.2 $[M+H]^+$.

LC-MS-MS condition for quantitative analysis

The analysis was performed using a UHPLC (Thermo Scientific Vanquish, MA, USA) equipped with VF-P10-A-01 binary pumps, VF-A10-A-02 split sampler, VH-C10-A-03 column compartment, VF-D11-A-01 diode array detector, and LTQ mass spectrometer (Thermo Scientific LTQ XL, MA, USA) through an ESI interface. All data were processed using the XCalibur program; the detailed analytical conditions for LC-MS/MS analysis of IBV compounds are shown in Table 1. The optimal parameters including collision energy (CE) are shown in Supplementary Table 1.

Preparation of samples and standard solutions for LC-MS analysis

Each of the eight compounds was accurately weighed and individually dissolved in a solvent mix (methanol 100%) at a concentration of 1.0 mg/mL. The individual standard solutions were stored at –20°C. Prior to LC-MS/MS analysis, equal volumes of each standard solution were mixed and diluted with the solvent to prepare a standard stock solution (50 μg/mL). The standard working solutions used for generating calibration curves, were prepared by appropriate dilution of the stock solution (0.05-2.5 μg/mL) in methanol (100%). The LC-MS/MS samples of *I. batatas* vine extracts were prepared in a solvent (methanol: water=1:1) at a concentration of 3.0 mg/mL. Dilutions were considered in the calculations of the final concentrations.

Cell culture

The human ovarian cancer cells (A2780) were purchased from Sigma Aldrich (St. Louis, MO, USA), maintained in a Roswell Park Memorial Institute (RPMI) 1640 medium (Cellgro, Manassas, VA, USA), supplemented with 1% penicillin/streptomycin (P/S; Gibco BRL, Carlsbad, MD, USA) and 10% fetal bovine serum (Gibco BRL, Carlsbad, MD, USA). The human umbilical vein endothelial cells (HUVECs) were purchased from American Type Culture Collection Manassas (ATCC; Manassas, VA, USA) and cultured using Clonetics EGM-2 MV BulletKit (Takara Bio Inc., Shiga, Japan). A2780 cells and HUVECs seeded in a 100 mm culture dish were maintained in incubators (37°C, humidified atmosphere with 5% CO_2 and 95% air).

Cell viability assay

Depending on the desired number of cells, the HepG2 cells (1×10^4 cells per well) and HUVECs (5×10^5 cells per well) are diluted in the medium and seeded in 96-well culture plates. After cultivation for 24 h, cells were treated with compounds **1-8** (6.2, 12.5, 25, 50, and 100 μM) for 24 h. Cells were treated with 0.5% DMSO in cell culture media as vehicle controls. After that, Ez-Cytox reagent (Daeil Lab Service Co., Seoul, Korea) measuring cell viability was added to each well. After cultivation for 1 h, the absorbance (490 nm) of produced dye was recorded using a PowerWave XS microplate reader (Bio-Tek Instruments, Winooski, VT, USA) to calculate the cell viability.

Tube formation

To coat the 96-well culture plates with Matrigel (BD Biosciences, San Jose, CA, USA), 10 mg/mL Matrigel was added to each well and incubated at 37°C for 30 min. The treatment of HUVECs (5×10^5 cells per well) was carried out with 1,3,5-tricaffeoylquinic acid (**5**) (25, 50, and 100 μM), U0126 (10 μM), and/or LY294002 (10 μM) for 24 h. A 4% paraformaldehyde solution (Sigma Aldrich) was added to each well, followed by hematoxylin (Muto Pure Chemicals, Tokyo, Japan) to stain the tubular structure formation in HUVECs. Tube length was inspected using a phase-contrast microscope at 200×magnification and quantified using the ImageJ software (version 1.48; National Institutes of Health, Bethesda, MD, USA). Data are expressed as the percentage increase in the total tube length of HUVECs.

Image-based cytometric assay

To do the image-based cytometric assay, the cultivation of A2780 cells (4×10^5 cells per well) was carried out in 6-well plates and the treatment was performed for 24 h at 50 and

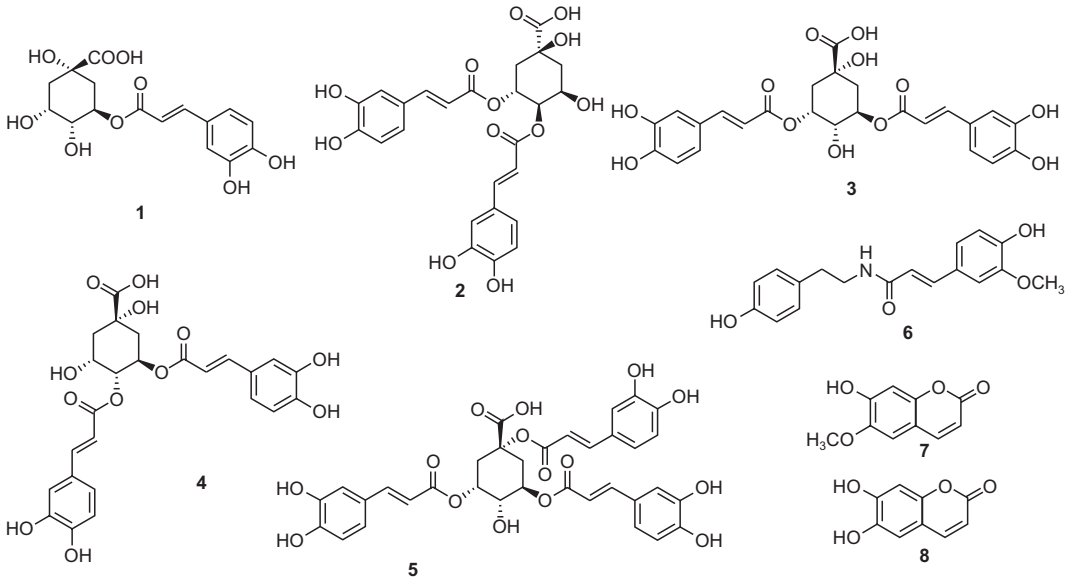

Fig. 1. Chemical structures of compounds **1-8**.

100 μM of 1,3,5-tricaffeoylquinic acid (**5**). Collected cells were washed with binding buffer (Life Technologies, Carlsbad, CA, USA) and stained in binding buffer with annexin V Alexa Fluor 488 (Invitrogen, Temecula, CA, USA). At last, incubation was performed for 30 min in dark, and annexin V-positive-stained apoptotic cells were determined by Tali image-based cytometer (Invitrogen).

Western blotting analysis

A sample of 20 μg total protein per lane were separated on 10% sodium dodecyl sulfate-polyacrylamide gel, transferred to polyvinylidene difluoride membranes (Pall Corporation, Washington, NY, USA), and probed with primary antibodies and secondary antibody (Cell Signaling, Boston, MA, USA). Primary antibody and secondary antibody were usually used at a dilution of 1:1000 and 1:2000, respectively. Visualization of immune complexes utilized chemiluminescence system (FUSION Solo; PEQLAB Biotechnologie GmbH, Erlangen, Germany). GAPDH was used to normalize the expression of the proteins.

Statistical analysis

Statistical analysis was performed using one-way analysis of variance and multiple comparisons with Bonferroni correction. Statistical significance was set at $p<0.05$. Data analyses were performed using the SPSS Statistics ver. 19.0 (SPSS Inc., Chicago, IL, USA).

RESULTS

Isolation and structural elucidation of compounds

Eight compounds were isolated and purified from *I. batatas* vines by stepwise chromatography in our laboratory, and their structures were elucidated by comparing their spectral data (UV, ^{1}H-NMR, and MS) with literature references: chlorogenic acid (**1**) (Zhao *et al*., 2014), 3,4-dicaffeoylquinic acid (**2**) (Zhao *et al*., 2014), 3,5-dicaffeoylquinic acid (**3**) (Zhao *et al*., 2014), 4,5-dicaffeoylquinic acid (**4**) (Zhao *et al*., 2014), 1,3,5-tricaffeoylquinic acid (**5**) (Cui *et al*., 2009), N-trans-feruoyltyramine (**6**) (Kanada *et al*., 2012), scopoletin (**7**) (Bhatt Mehul *et al*., 2011), and esculetin (**8**) (Kim *et al*., 2000). Chlorogenic acid (**1**) is an ester of caffeic acid and (−)-quinic acid. All the compounds are shown in Fig. 1. To the best of our knowledge, compound **5**, 1,3,5-tricaffeoylquinic acid, was isolated for the first time from this plant.

HPLC-UV and LC-MS-MS condition for the extracts and compounds

The HPLC-DAD profile of the *I. batatas* vine extracts showed eight peaks. Chlorogenic acid (**1**) appeared at Rt 3.9 min whereas compounds **2**, **3**, and **4** appeared at Rt 8.1, 7.4, and 7.1 min, respectively. Reverse-phase HPLC with DAD detection was successfully able to separate chlorogenic acid (**1**) and its derivatives (**2-5**). The purity of the isolated compounds was determined using a diode array detector. Six standard compounds were isolated from each other at each time point in one peak. The identities of standard compounds in the extract of *I. batatas* vines were confirmed by injecting crude samples with each standard compound, which supported the specificity of each peak. In the UHPLC-ESI-MS/MS spectra, each molecular ion and fragmentation pattern of each compound matched well with the respective chemical structure (Supplementary Table 1).

Optimization and validation of the method. To achieve the best separation and strong ion signals, the chromatographic conditions, including the mobile phase, column temperature, and flow rate, were optimized. Different linear gradients of mobile phases A and B, different columns, and different flow rates of the solvent gradient were compared (data not shown). The chromatographic conditions that yielded the best base-line separation of closely related chlorogenic acid derivatives were water with 0.1% formic acid (A) and acetonitrile with 0.1% formic acid (B) as the eluents, with a flow rate of 0.3 mL/min, and

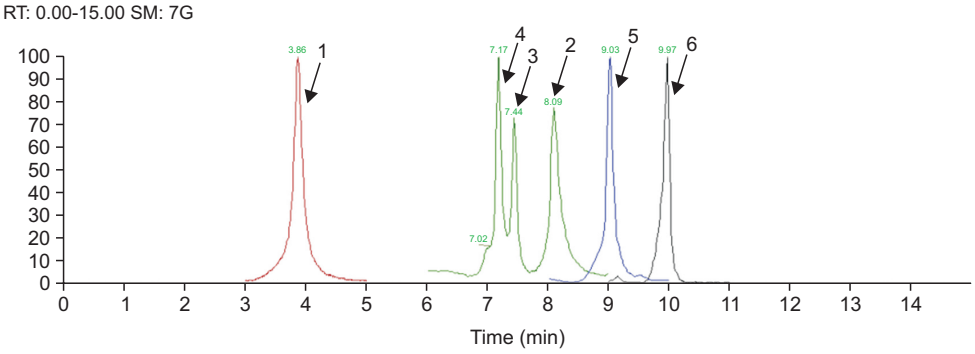

Fig. 2. MS/MS Chromatogram of *Ipomoea batatas* vine extracts (SIM). Chlorogenic acid (**1**, 3.86 min); 4,5-dicaffeoylquinic acid (**4**, 7.17 min); 3,5-dicaffeoylquinic acid (**3**, 7.44 min); 3,4-dicaffeoylquinic acid (**2**, 8.09 min); 1,3,5-tricaffeoylquinic acid (**5**, 9.03 min); *N-trans*-feruoyltyramine (**6**, 9.97 min).

Table 2. Regression equation, correlation coefficients, LOD and LOQ for compounds **1-6**

No.	Regression equation	Correlation coefficient	LOD (ng/mL)	LOQ (ng/mL)	Contents (μg/g extracts)	
					Mean	RSD (%)
1	Y=152.206X+4153.51	0.9997	1.04	3.15	407.77	3.73
2	Y=31.6698X+1533.11	0.9994	2.68	8.13	648.85	1.81
3	Y=32.9196X+85.3884	0.9999	1.60	4.85	450.57	3.26
4	Y=45.8209X-25.8824	0.9997	2.17	6.58	677.43	1.25
5	Y=59.576X+131.283	0.9997	1.86	5.64	7.72	13.2
6	Y=7.82153X+99.2912	0.9998	3.61	10.94	15.4	9.61

a column temperature of 30°C. Because of the complexity of IBV extracts, a detailed gradient program was employed. The typical separation of the extracted ion chromatograms (EIC) of the standard reference mixture and IBV sample is shown in Fig. 2.

Specificity, linearity, accuracy, precision, range, quantitation limits, and detection limits were determined according to the FDA Guidance for Industry. Standard compound calibration curves comprised six concentration levels (0.05-2.5 μg/mL), and each concentration was prepared and assayed in five runs on three separate days. The ratios of the peak area of the analytes to those of the internal standard were plotted against the nominal analyte concentrations, and the standard curves were in the form of Y=aX+b. The regression coefficients (r^2), and linear regression equations of compounds are presented in Table 2.

IBV extracts were run using the LC-LTQ-MS/MS validated method for simultaneous quantification of six phenolic compounds. Five chlorogenic acid derivatives and one feruloyl derivative were quantified. Compounds **2** and **4** were the most abundant, and compounds **1** and **3** were more than half of compounds **2** and **4** in the sample. Further, compound **5** was detected using LC-ESI-MS/MS; however, only trace amounts were detected in this investigation. Compound **6** was present at a low concentration in the sample (15.4 μg/g).

Effects of the isolated compounds 1-8 on the viability of A2780 cells

We determined whether compounds **1-8** showed cytotoxic in A2780 cells and examined their effects on A2780 cell viability (Fig. 3) using an Ez-Cytox cell viability assay. Compounds **1-8** showed cytotoxic effects against A2780 cells, resulting in decreased cell viability (45.91 ± 1.23% for **1**, 67.01 ± 2.33% for **2**, 42.66 ± 3.55% for **3**, 60.61 ± 4.64% for **4**, 25.81 ± 1.79% for **5**, 68.51 ± 2.71% for **6**, 56.12 ± 4.95% for **7**, and 55.29 ± 2.04% for **8**) at 100 μM. The IC50 values of **1**, **3**, and **5** were 80.97 ± 2.01, 80.05 ± 3.85, and 47.43 ± 2.43 μM, respectively (Fig. 3). Among the isolated compounds, 1,3,5-tricaffeoylquinic acid (**5**) exhibited the highest concentration-dependent cytotoxicity against A2780 cells (Fig. 3). Thus, 1,3,5-tricaffeoylquinic acid (**5**) was selected for the subsequent experiments.

Effects of 1,3,5-tricaffeoylquinic acid (5) on apoptosis signaling pathways in A2780 cells

Image-based cytometric analysis was performed to evaluate whether treatment with 1,3,5-tricaffeoylquinic acid (**5**) could increase the number of Annexin V- stained apoptotic cells. After treatment with 1,3,5-tricaffeoylquinic acid (**5**) (50 and 100 μM), A2780 cells were stained with Annexin V Alexa Fluor 488. The results showed that 1,3,5-tricaffeoylquinic acid (**5**) induces apoptotic death in A2780 cells. As shown in Fig. 4, the percentage of Annexin V-positive cells, indicating apoptotic cell death was significantly increased to 15.63% ± 1.06% and 37.81% ± 2.26% by treatment with 1,3,5-tricaffeoylquinic acid (**5**) (50 and 100 μM), compared to that in the control (1.91 ± 0.21%).

Next, we performed Western blotting to evaluate the molecular pathways activated by 1,3,5-tricaffeoylquinic acid (**5**) to induce apoptosis in A2780 cells. Treatment with 1,3,5-tricaffeoylquinic acid (**5**) (50 and 100 μM) increased the protein expression levels of cleaved caspase-8, Bcl-2-associated X protein (Bax), cleaved caspase-9, cleaved caspase-3, and

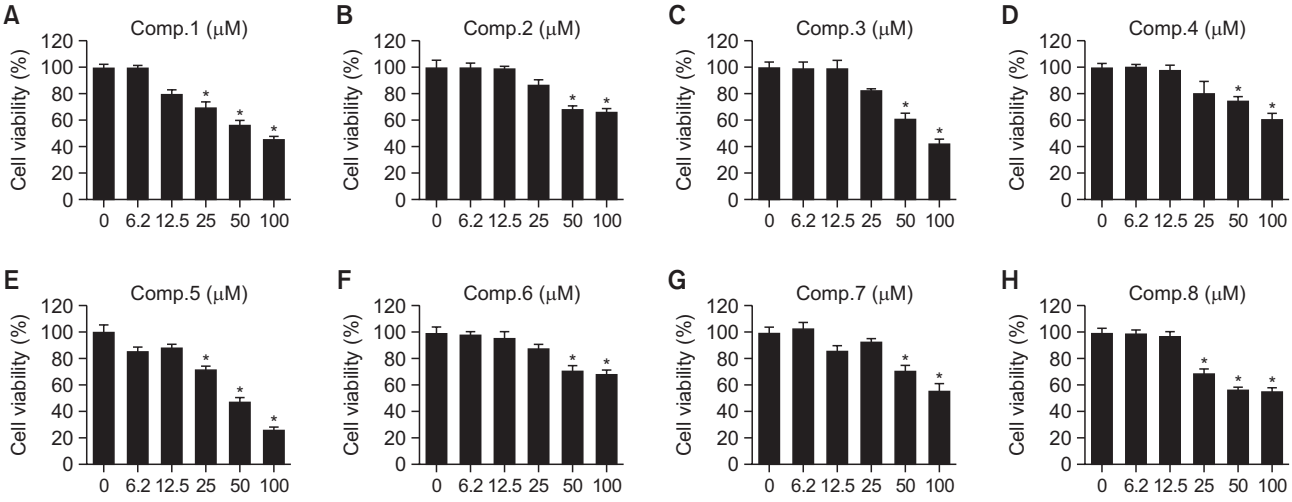

Fig. 3. Effects of compounds **1-8** on human ovarian cancer (A2780) cell viability. A2780 cells were treated with compounds **1** (A), **2** (B), **3** (C), **4** (D), **5** (E), **6** (F), **7** (G), and **8** (H) (6.2, 12.5, 25, 50, and 100 μM) for 24 h. A2780 cells were treated with 0.5% DMSO in cell culture media as vehicle controls. The viability of A2780 cells was assessed using the Ez-Cytox cell viability assay. Data are presented as the mean ± standard error of the mean (SEM). n=3, **p*<0.05 compared with the control.

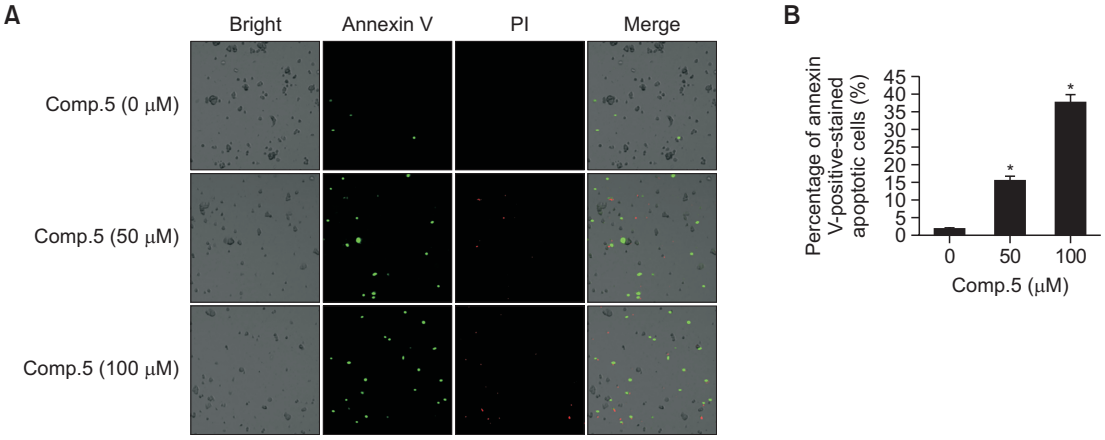

Fig. 4. Effects of 1,3,5-tricaffeoylquinic acid (**5**) on apoptotic death in human ovarian cancer (A2780) cells. A2780 cells were treated with 1,3,5-tricaffeoylquinic acid (**5**) (50 and 100 μM) for 24 h. A2780 cells were treated with 0.5% DMSO in cell culture media as vehicle controls: (A) Visualization of apoptotic cells stained with Annexin V (40× magnification). (B) Bar graph representing percentage of apoptotic cells. Data are presented as the mean ± standard error of the mean (SEM). n=3, **p*<0.05 compared with the control.

cleaved poly (ADP-ribose) polymerase (cleaved PARP), and decreased the expression of B-cell lymphoma 2 (Bcl-2) (Fig. 5).

Effects of 1,3,5-tricaffeoylquinic acid on HUVEC tube formation

First, non-toxic concentrations of 1,3,5-tricaffeoylquinic acid (**5**) were determined using a cell viability assay and were then applied to HUVECs. HUVEC viability was assessed using the MTT assay in HUVECs treated with 1,3,5-tricaffeoylquinic acid (**5**) (25, 50, and 100 μM), U0126 (10 μM), or LY294002 (10 μM) for 24 h. None of these combinations or single treatments affected HUVEC viability (Fig. 6A). These nontoxic concentrations were thus used in the tube formation assay. When HUVECs were cultured with 1,3,5-tricaffeoylquinic acid (**5**) (25, 50, and 100 μM), tube formation was reduced by 85.75 ± 1.54 and 61.77 ± 4.07% at 50 μM and 100 μM, respectively. These effects were enhanced by co-treatment with a mitogen-activated protein kinase (MEK)/extracellular signal-regulated kinase (ERK) inhibitor (U0126) or phosphatidylinositol 3-kinase (PI3K) inhibitor (LY294002). Incubation of HUVECs with 100 μM 1,3,5-tricaffeoylquinic acid (**5**) and 10 μM U0126 reduced tube formation by 64.93 ± 2.41%. Treatment with 100 μM 1,3,5-tricaffeoylquinic acid (**5**) and 10 μM LY294002 reduced tube formation by 45.43 ± 2.75% (Fig. 6B, 6C).

Effects of 1,3,5-tricaffeoylquinic acid on the vascular endothelial growth factor receptor (VEGFR) 2 signaling pathway in HUVECs

Western blotting was performed to evaluate the potential molecular mechanisms by which 1,3,5-tricaffeoylquinic acid (**5**) inhibited HUVEC tube formation. Treatment with 1,3,5-tri-

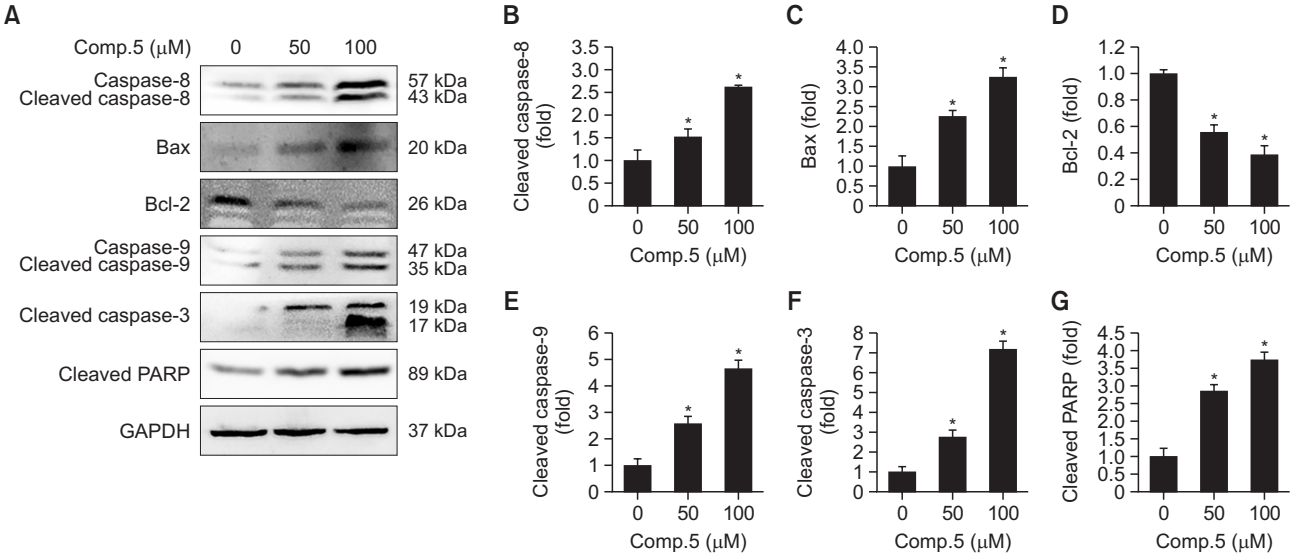

Fig. 5. Effects of 1,3,5-tricaffeoylquinic acid (**5**) on apoptosis signaling pathways in human ovarian cancer (A2780) cells. A2780 cells were treated with 1,3,5-tricaffeoylquinic acid (**5**) (50 and 100 μM) for 24 h. A2780 cells were treated with 0.5% DMSO in cell culture media as vehicle controls: (A) Protein expression levels of cleaved caspase-8, Bcl-2-associated X protein (Bax), B-cell lymphoma 2 (Bcl-2), cleaved caspase-9, cleaved caspase-3, cleaved poly (ADP-ribose) polymerase (cleaved PARP), and glyceraldehyde-3-phosphate dehydrogenase (GAPDH). (B-G) Each bar graph presents the densitometric quantification of protein expression levels. Data are presented as the mean ± standard error of the mean (SEM). n=3, **p*<0.05 compared with the control.

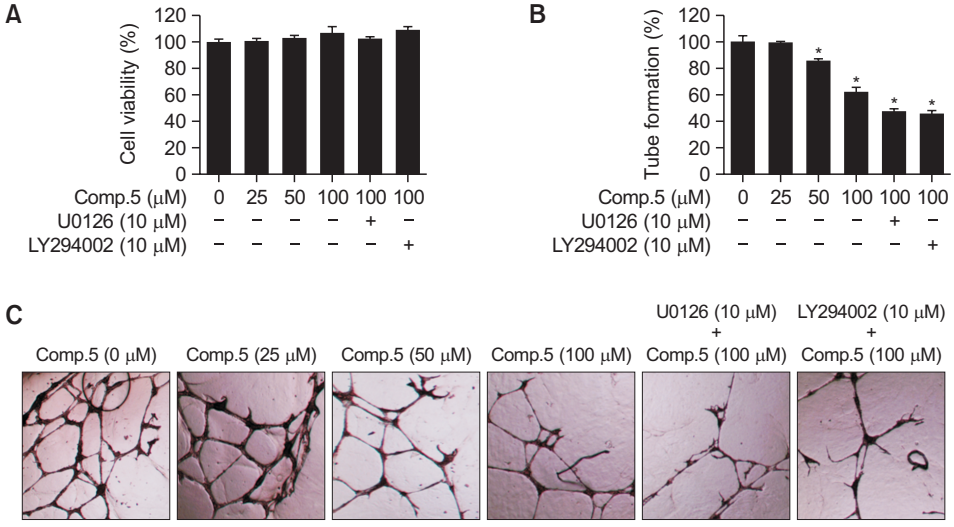

Fig. 6. Effects of 1,3,5-tricaffeoylquinic acid (**5**) on cell viability and tube formation in human umbilical vein endothelial cells (HUVECs). HUVECs were treated with 1,3,5-tricaffeoylquinic acid (**5**) (25, 50, and 100 μM), mitogen-activated protein kinase (MEK)/extracellular signal-regulated kinase (ERK) inhibitor (U0126) (10 μM), and/or phosphatidylinositol 3-kinase (PI3K) inhibitor (LY294002) (10 μM) for 24 h. HUVECs were treated with 0.5% DMSO in cell culture media as vehicle controls: (A) The viability of HUVECs was assessed using the Ez-Cytox cell viability assay. (B) Representative photographs of HUVEC tube formation on Matrigel at 200× magnification. (C) The relative lengths of tubes were quantified using ImageJ software. Data are presented as the mean ± standard error of the mean (SEM). n=3, **p*<0.05 compared with the control.

caffeoylquinic acid (**5**) (50 and 100 μM) decreased VEGFR2 phosphorylation (Fig. 7A, 7B). Treatment with 1,3,5-tricaffeoylquinic acid (**5**) (50 and 100 μM) also reduced ERK phosphorylation. This effect was enhanced by co-treatment with 10 μM of U0126 (Fig. 7C, 7D). Treatment with 1,3,5-tricaffeoylquinic acid (**5**) (50 and 100 μM) decreased the phosphorylation of phosphoinositide 3-kinase (PI3K), Akt, and mammalian target of rapamycin (mTOR), which was enhanced upon co-treatment with 10 μM LY294002 (Fig. 7E-7H). These results indicate the potential mechanism of action by which 1,3,5-tricaffeoylquinic acid (**5**) can inhibit angiogenesis by HUVECs.

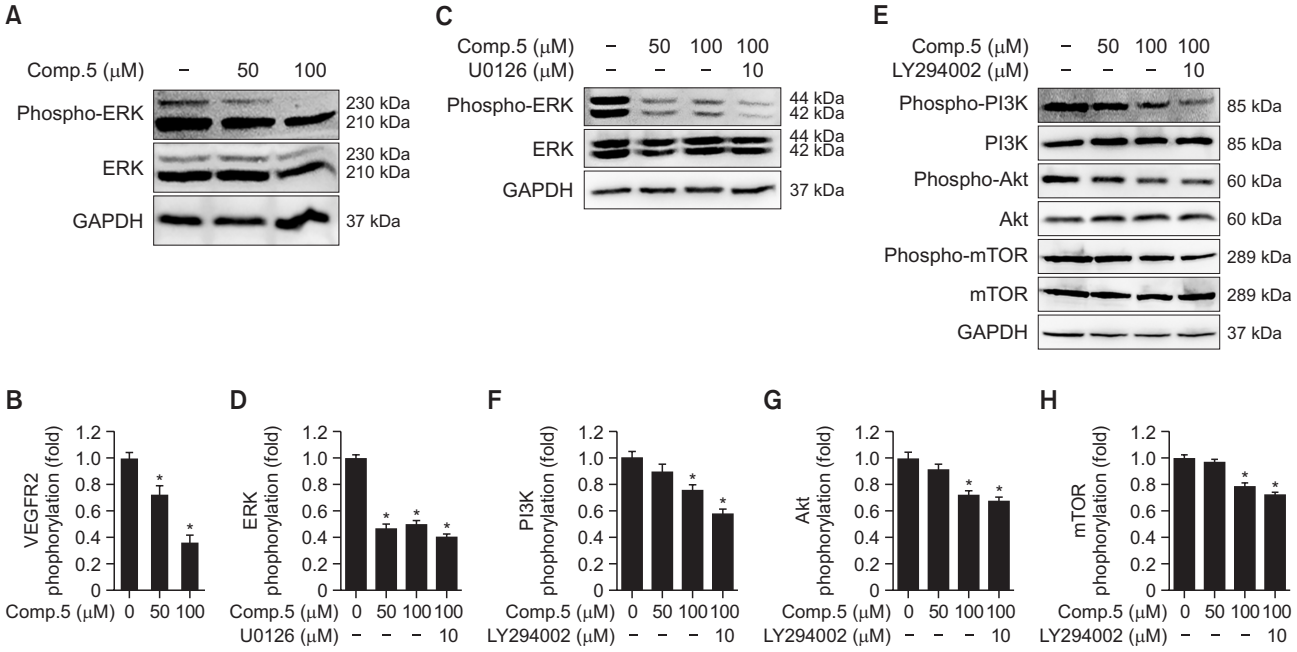

Fig. 7. Effects of 1,3,5-tricaffeoylquinic acid (**5**) on the vascular endothelial growth factor receptor 2 (VEGFR2) signaling pathway in human umbilical vein endothelial cells (HUVECs). HUVECs were treated with 1,3,5-tricaffeoylquinic acid (**5**) (50 and 100 μM), mitogen-activated protein kinase (MEK)/extracellular signal-regulated kinase (ERK) inhibitor (U0126) (10 μM), and/or phosphatidylinositol 3-kinase (PI3K) inhibitor (LY294002) (10 μM) for 24 h. HUVECs were treated with 0.5% DMSO in cell culture media as vehicle controls. Protein expression levels of (A, B) phospho-VEGFR2), VEGFR2, (C, D) Phospho-ERK, ERK, (E-H) Phospho-PI3K, PI3K, phospho-Akt, Akt, phospho-mammalian target of rapamycin (Phospho-mTOR), mTOR, and glyceraldehyde-3-phosphate dehydrogenase (GAPDH). Each bar graph presents the densitometric quantification of protein expression levels. Data are presented as the mean ± standard error of the mean (SEM). n=3, **p*<0.05 compared with the control.

DISCUSSION

Ovarian cancer development has been related to dysregulation of programmed cell death or apoptosis (Al-Alem *et al*., 2019). Apoptosis is precisely controlled to remove the dangerous, damaged, aged, and infected cells in an orderly manner (Maiuri *et al*., 2007). Apoptosis interferes with cancer growth via activation of the caspase-mediated extrinsic or intrinsic pathway (Hu and Kavanagh, 2003). This study demonstrates that 1,3,5-tricaffeoylquinic acid (**5**) can decrease the viability of and induce apoptosis in A2780 human ovarian cancer cells. The effects of 1,3,5-tricaffeoylquinic acid (**5**) on intracellular signaling pathways related to apoptosis were investigated by western blot analysis. In the extrinsic apoptosis pathway, 1,3,5-tricaffeoylquinic acid (**5**) induced caspase-8 activation. In the intrinsic apoptosis pathway, 1,3,5-tricaffeoylquinic acid (**5**) induces the activation of pro-apoptotic Bax proteins, along with concomitant inhibition of anti-apoptotic Bcl-2 proteins and cleavage of caspase-9. Bcl-2 family proteins (Bax and Bcl-2) regulate the release of cytochrome c from mitochondria, thus activating caspase-9 (Scorrano and Korsmeyer, 2003). Both the caspase-8 and caspase-9 stimulate caspase-3 activation, resulting in altered levels of downstream PARP cleavage (Aouad *et al*., 2004). Upon DNA damage, PARP is rapidly activated and binds to DNA. Eventually it accelerates cell death after DNA damage-induced apoptosis (Beneke *et al*., 2000). We thus observed that 1,3,5-tricaffeoylquinic acid (**5**) activated the cleavage of caspase-3 and PARP. Therefore, both caspase-mediated extrinsic or intrinsic pathways might be implicated in apoptosis induced by 1,3,5-tricaffeoylquinic acid (**5**) (Fig. 8).

Ovarian cancer usually metastasizes from the ovary to adjacent organs through direct invasion of blood vessels, which are composed of endothelial cells (Naora and Montell, 2005). Angiogenesis, the process of new blood vessel formation from preexisting vessels, is a vital process during cancer metastases (Pradeep *et al*., 2005). The tube formation assay using HUVECs has been known as a routinely used and reliable *in vitro* experimental model to evaluate anti-angiogenic potential (DeCicco-Skinner *et al*., 2014; Gentile *et al*., 2019). In the present study, we report 1,3,5-tricaffeoylquinic acid (**5**) as an inhibitor of angiogenesis. We found that 1,3,5-tricaffeoylquinic acid (**5**) inhibited capillary structure formation in HUVECs. Further, co-treatment with ERK and PI3K inhibitors enhanced the inhibitory potency of 1,3,5-tricaffeoylquinic acid (**5**) on capillary structure formation in HUVECs. These results indicate that 1,3,5-tricaffeoylquinic acid (**5**) modulated angiogenesis by inhibiting ERK and PI3K. VEGFR2 is both an angiogenic stimulator and an upstream signal of ERK and PI3K pathway relevant to angiogenesis (Karar and Maity, 2011; Jin *et al*., 2018). In the present study, 1,3,5-tricaffeoylquinic acid (**5**) suppressed the phosphorylation of VEGFR2 as well as ERK and PI3K. ERK is known to contribute to the proliferation of umbilical vein endothelial cells during angiogenesis (Wu *et al*., 2015). Previously, activated PI3K/Akt has been reported to regulate a downstream molecule, mTOR, to increase the proliferation of umbilical vein endothelial cells (Tsuji-Tamura *et al*., 2020). Further, mTOR inhibitors delay cancer metasta-

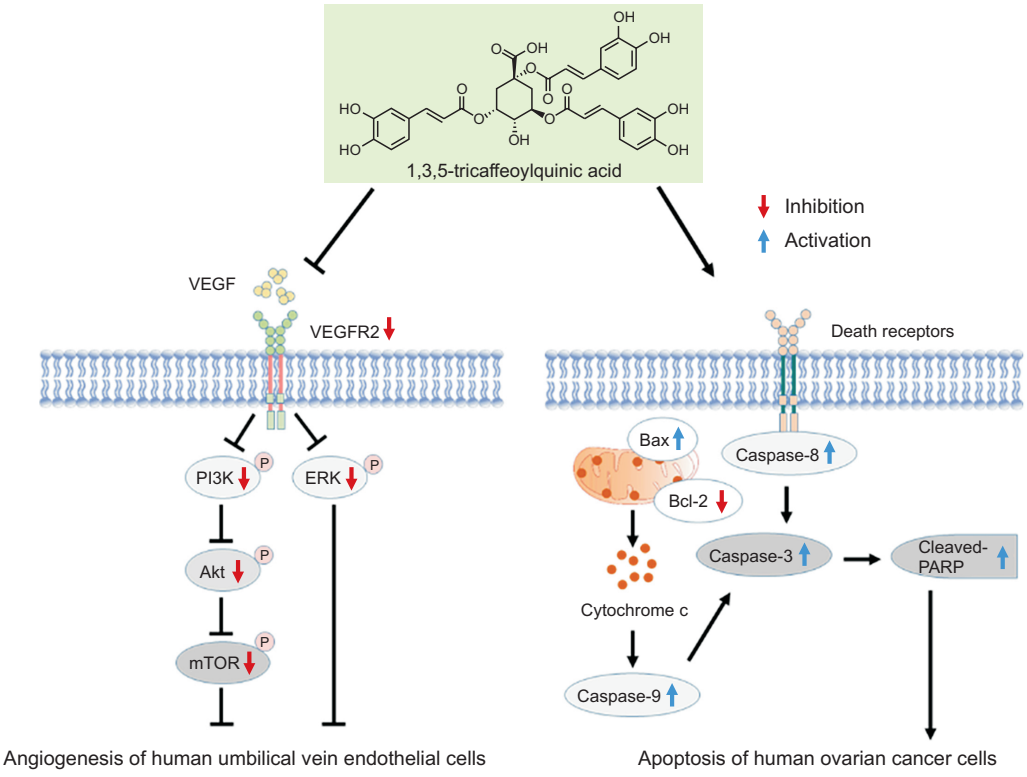

Fig. 8. Schematic pathway illustrating the potential role of 1,3,5-tricaffeoylquinic acid (**5**) in human ovarian cancer cell apoptosis and tube formation in human umbilical vein endothelial cells. VEGFR2, vascular endothelial growth factor receptor 2; ERK, extracellular signalregulated kinase; PI3K, phosphoinositide 3-kinase; mTOR, Bax, Bcl-2-associated X protein; cleaved PARP, cleaved poly (ADP-ribose) polymerase.

ses partly by inhibiting angiogenic processes (Lamanuzzi *et al*., 2018). In the present study, 1,3,5-tricaffeoylquinic acid (**5**) suppressed the phosphorylation of PI3K/Akt as well as mTOR. Taken together, our results suggest that 1,3,5-tricaffeoylquinic acid (**5**) inhibits tubular structure formation by inhibiting VEGFR2 phosphorylation and its downstream signaling pathways in HUVECs (Fig. 6). Consequently, the findings of the present study warrant further investigation on the anticancer effect of 1,3,5-tricaffeoylquinic acid (**5**) in using mouse models of ovarian cancer and angiogenesis. Natural products provide a complementary strategy to existing ovarian cancer therapies by enhancing efficacy, mitigating side effects, and targeting cancer through multiple mechanisms. Resistance to standard treatments is common in ovarian cancer, necessitating alternative approaches such as therapies that induce apoptosis or inhibit angiogenesis to overcome resistance (Monk *et al*., 2016). Plant-derived compounds, such as withanolide glycosides and gintonin, have demonstrated anti-tumor effects through apoptosis induction, cell cycle arrest, and angiogenesis inhibition (Lee *et al*., 2022; Kim *et al*., 2023). However, few compounds exhibit multi-targeted actions against tumors. Anti-angiogenic agents can potentiate chemotherapy or targeted therapies by normalizing tumor vasculature, improving drug delivery, and activating apoptotic pathways. For instance, betulinic acid induces hypoxia like as 1,3,5-tricaffeoylquinic acid, which can trigger both caspase-mediated extrinsic and intrinsic pathways in tumor cells (Kutkowska *et al*., 2021). Nevertheless, the cellular responses to this compound may not fully replicate the pharmacokinetics, metabolism, and toxicity seen *in vivo*, necessitating comprehensive pharmacokinetic studies and long-term stability evaluations.

Compounds from purple sweet potato tubers can be identified and quantified using a variety of analytical techniques. For instance, mono-, di-, and tri-caffeoyl quinic acids, which are derivatives of chlorogenic acid, have been extracted and quantified by HPLC-UV from the leaves of *I. batatas* (Islam *et al*., 2002). LC-ESI-MS-MS-based simultaneous quantification method was first developed and employed in this study.

CONFLICT OF INTEREST

The authors declare that they have no known competing financial interests or personal relationships that could have appeared to influence the work reported in this paper.

ACKNOWLEDGMENTS

This research was supported by the National Research Foundation of Korea (NRF-2021R1A2C1004958 and NRF-2022R1A4A3022401).

AUTHOR CONTRIBUTIONS

Jaekyoung Kim: Methodology, validation, writing–original draft. Dahae Lee: investigation, validation, writing–original draft. Jin Woo Lee: data analysis. Changyeol Lee: data analysis. Ki Sung Kang: conceptualization, funding acquisition, methodology, writing – review and editing. Sang Hee Shim: methodology, supervision, funding acquisition, writing – review and editing.

ASSOCIATED CONTENT

Supporting Information

Supporting Information is available free of charge on the website at DOI: https://doi.org/10.4062/biomolther.2024.239. NMR and MS spectra of compounds **1-8**.

ORCID

Sang Hee Shim: 0000-0002-0134-0598

REFERENCES

Al-Alem, L. F., Baker, A. T., Pandya, U. M., Eisenhauer, E. L. and Rueda, B. R. (2019) Understanding and targeting apoptotic pathways in ovarian cancer. *Cancers (Basel)* **11**, 1631.

Aouad, S. M., Cohen, L. Y., Sharif-Askari, E., Haddad, E. K., Alam, A. and Sekaly, R.-P. (2004) Caspase-3 is a component of Fas death-inducing signaling complex in lipid rafts and its activity is required for complete caspase-8 activation during Fas-mediated cell death. *J. Immunol.* **172**, 2316-2323.

Beneke, R., Geisen, C., Zevnik, B., Bauch, T., Muller, W. U., Kupper, J. H. and Moroy, T. (2000) DNA excision repair and DNA damage-induced apoptosis are linked to poly(ADP-ribosyl)ation but have different requirements for p53. *Mol. Cell. Biol.* **20**, 6695-6703.

Bhatt Mehul, K., Dholwani Kishor, K. and Saluja Ajay, K. (2011) Isolation and structure elucidation of scopoletin from Ipomoea reniformis (Convolvulaceae). *J. Appl. Pharm. Sci.* **1**, 138-144.

Cui, C. B., Jeong, S. K., Lee, Y. S., Lee, S. O., Kang, I. J. and Lim, S. S. (2009) Inhibitory activity of caffeoylquinic acids from the aerial parts of Artemisia princes on rat lens aldose reductase and on the formation of advanced glycation end products. *J. Korean Soc. Appl. Biol. Chem.* **52**, 655-662.

DeCicco-Skinner, K. L., Henry, G. H., Cataisson, C., Tabib, T., Gwilliam, J. C., Watson, N. J., Bullwinkle, E. M., Falkenburg, L., O'Neill, R. C. and Morin, A. (2014) Endothelial cell ube formation assay for the *in vitro* study of angiogenesis. *J. Vis. Exp.* **91**, e51312.

Doubeni, C. A., Doubeni, A. R. and Myers, A. E. (2016) Diagnosis and management of ovarian cancer. *Am. Fam. Physician* **93**, 937-944.

Gentile, M. T., Pastorino, O., Bifulco M. and Colucci-D'Amato, L. (2019) HUVEC tube-formation assay to evaluate the impact of natural products on angiogenesis. *J. Vis. Exp.* **148**, e58591.

Hu, W. and Kavanagh, J. J. (2003) Anticancer therapy targeting the apoptotic pathway. *Lancet Oncol.* **4**, 721-729.

Islam, M. S., Yoshimoto, M., Yahara, S., Okuno, S., Ishiguro, K. and Yamakawa, O. (2002) Identification and characterization of foliar polyphenolic composition in sweetpotato (*Ipomoea batatas* L.) genotypes. *J. Agric. Food Chem.* **50**, 3718-3722.

Jiang, T., Ye, S., Liao, W., Wu, M., He, J., Mateus, N. and Oliveira, H. (2022) The botanical profile, phytochemistry, biological activities and protected-delivery systems for purple sweet potato (*Ipomoea batatas* (L.) Lam.): an up-to-date review. *Food Res. Int.* **161**, 111811.

Jin, F., Xie, T., Huang, X. and Zhao, X. (2018) Berberine inhibits angiogenesis in glioblastoma xenografts by targeting the VEGFR2/ERK pathway. *Pharm. Biol.* **56**, 665-671.

Kanada, R. M., Simionato, J. I., Arruda, R. F. D., Santin, S. M. D. O., Souza, M. C. D. and Silva, C. C. D. (2012) N-trans-feruloyltyramine and flavonol glycosides from the leaves of Solanum sordidum. *Rev. Bras. Farmacogn.* **22**, 502-506.

Karar, J. and Maity, A. (2011) PI3K/AKT/mTOR pathway in angiogenesis. *Front. Mol. Neurosci.* **4**, 51.

Kim, N. M., Kim, J., Chung, H. Y. and Choi, J. S. (2000) Isolation of luteolin 7-O-rutinoside and esculetin with potential antioxidant activity from the aerial parts of *Artemisia montana*. *Arch. Pharm. Res.* **23**, 237-239.

Kim, S. J., Nah, S. Y., Park, I. H., Shin, M. S. and Kang, K. S. (2023) Gintonin isolated from ginseng inhibits the epithelial-mesenchymal transition induced by TGF-beta in A549 lung cancer cells. *Plants* **12**, 2013.

Kutkowska, J., Strzadala, L. and Rapak, A. (2021) Hypoxia increases the apoptotic response to betulinic acid and betulin in human non-small cell lung cancer cells. *Chem. Biol. Interact.* **333**, 109320.

Lamanuzzi, A., Saltarella, I., Desantis, V., Frassanito, M. A., Leone, P., Racanelli, V., Nico, B., Ribatti, D., Ditonno, P., Prete, M., Solimando, A. G., Dammacco, F., Vacca, A. and Ria, R. (2018) Inhibition of mTOR complex 2 restrains tumor angiogenesis in multiple myeloma. *Oncotarget* **9**, 20563-20577.

Lee, D., Yu, J. S., Ha, J. W., Lee, S. R., Lee, B. S., Kim, J. C., Kim, J. K., Kang, K. S. and Kim, K. H. (2022) Antitumor potential of withanolide glycosides from Ashwagandha (Withaniasomnifera) on apoptosis of human hepatocellular carcinoma cells and tube formation in human umbilical vein endothelial cells. *Antioxidants* **11**, 1761.

Maiuri, M. C., Zalckvar, E., Kimchi, A. and Kroemer, G. (2007) Self-eating and self-killing: crosstalk between autophagy and apoptosis. *Nat. Rev. Mol. Cell Biol.* **8**, 741-752.

Markman, M., Webster, K., Zanotti, K., Peterson, G., Kulp, B. and Belinson, J. (2004) Survival following the documentation of platinum and taxane resistance in ovarian cancer: a single institution experience involving multiple phase 2 clinical trials. *Gynecol. Oncol.* **93**, 699-701.

Mohanraj, R. and Sivasankar, S. (2014) Sweet potato (*Ipomoea batatas* [L.] Lam)-a valuable medicinal food: a review. *J. Med. Food* **17**, 733-741.

Monk, B. J., Herzog, T. J. and Tewari, K. S. (2016) Evolution of chemosensitivity and resistance assays as predictors of clinical outcomes in epithelial ovarian cancer patients. *Curr. Pharm. Des.* **22**, 4717-4728.

Naora, H. and Montell, D. J. (2005) Ovarian cancer metastasis: integrating insights from disparate model organisms. *Nat. Rev. Cancer* **5**, 355-366.

Noumi, E. (2010) Ethno medicines used for treatment of prostatic disease in Foumban, Cameroon. *Afr. J. Pharmacy Pharmacol.* **4**, 793-805.

Pezzuto, J. M. (1997) Plant-derived anticancer agents. *Biochem. Pharmacol.* **53**, 121133.

Pistollato, F., Giampieri, F. and Battino, M. (2015) The use of plant-derived bioactive compounds to target cancer stem cells and modulate tumor microenvironment. *Food Chem. Toxicol.* **75**, 58-70.

Pradeep, C., Sunila, E. and Kuttan, G. (2005) Expression of vascular endothelial growth factor (VEGF) and VEGF receptors in tumor angiogenesis and malignancies. *Integr. Cancer Ther.* **4**, 315-321.

Reed, J. C. (2002) Apoptosis-based therapies. *Nat. Rev. Drug Discov.* **1**, 111-121.

Roy, A., Datta, S., Bhatia, K. S., Jha, P. and Prasad, R. (2021) Role of plant derived bioactive compounds against cancer. *S. African J. Bot.* **149**, 1017-1028.

Scappaticci, F. A. (2002) Mechanisms and future directions for angiogenesis-based cancer therapies. *J. Clin. Oncol.* **20**, 3906-3927.

Scorrano, L. and Korsmeyer, S. J. (2003) Mechanisms of cytochrome c release by proapoptotic BCL-2 family members. *Biochem. Biophys. Res. Commun.* **304**, 437-444.

Tsuji-Tamura, K., Sato, M., Fujita, M. and Tamura, M. (2020) The role of PI3K/Akt/mTOR signaling in dose-dependent biphasic effects of glycine on vascular development. *Biochem. Biophys Res. Commun.* **529**, 596-602.

Wu, F., Song, H., Zhang, Y., Zhang, Y., Mu, Q., Jiang, M., Wang, F., Zhang, W., Li, L. and Li, H. (2015) Irisin induces angiogenesis in human umbilical vein endothelial cells *in vitro* and in zebrafish embryos *in vivo* via activation of the ERK signaling pathway. *PLoS One* **10**, e0134662.

Zanetta, G., Chiari, S., Rota, S., Bratina, G., Maneo, A., Torri, V. and Mangioni, C. (1997) Conservative surgery for stage I ovarian carcinoma in women of childbearing age, BJOG-Int. *J. Obstet. GY.* **104**, 1030-1035.

Zhang, C., Liu, D., Wu, L., Zhang, J., Li, X. and Wu, W. (2019) Chemical characterization and antioxidant properties of ethanolic extract and its fractions from sweet potato (*Ipomoea batatas* L.) leaves. *Foods* **9**, 15.

Zhao, J. G., Yan, Q. Q., Xue, R. Y., Zhang, J. and Zhang, Y. Q. (2014) Isolation and identification of colourless caffeoyl compounds in purple sweet potato by HPLC-DAD–ESI/MS and their antioxidant activities. *Food Chem.* **161**, 22-26.